iScience, Volume *26*

Supplemental information

Phenotypic and functional characterization of pharmacologically expanded Vγ9Vδ2 T cells in pigtail macaques

Isaac M. Barber-Axthelm, Kathleen M. Wragg, Robyn Esterbauer, Thakshila H. Amarasena, Valerie R.B. Barber-Axthelm, Adam K. Wheatley, Anne M. Gibbon, Stephen J. Kent, and Jennifer A. Juno

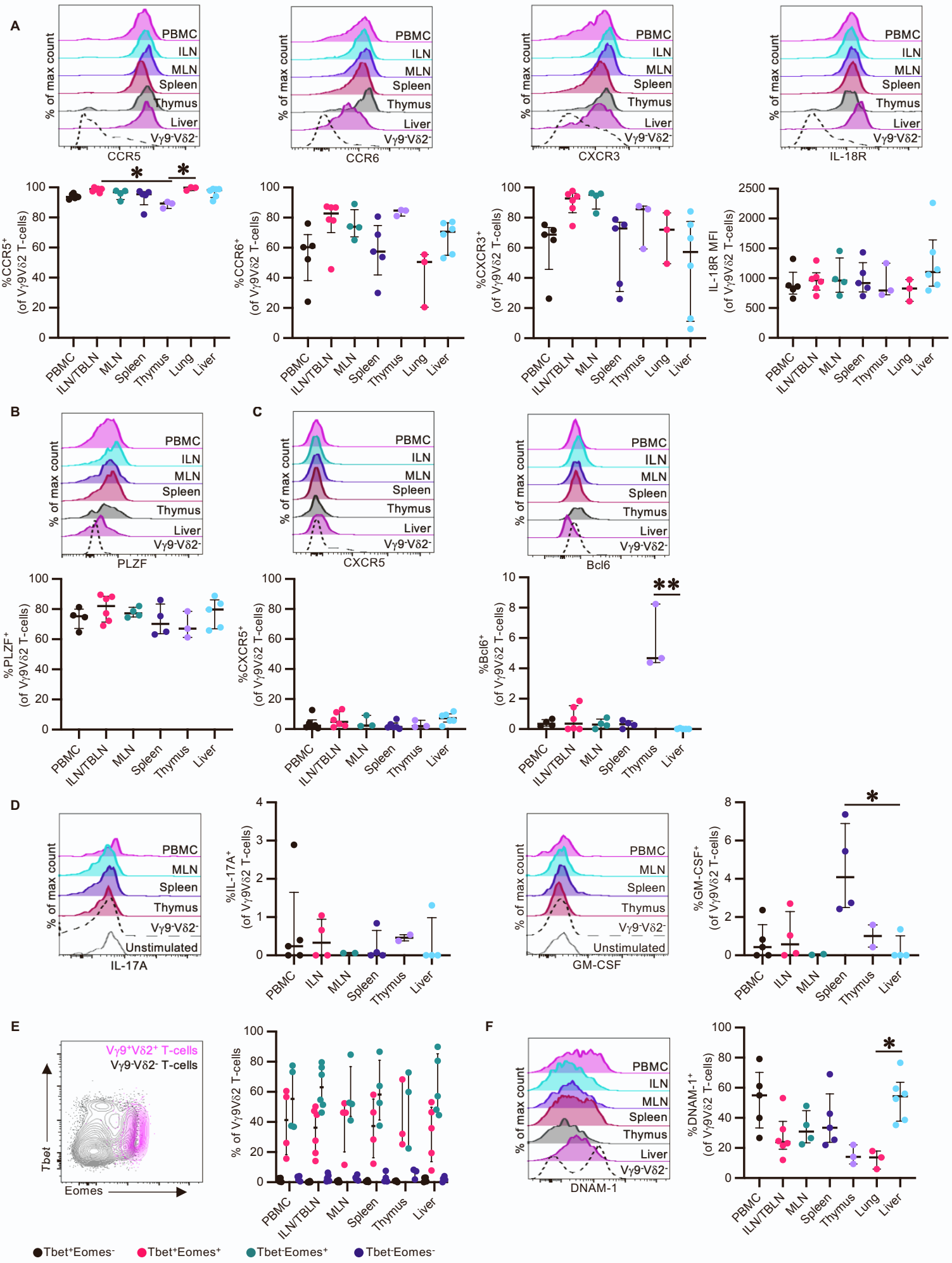

Figure S1: Vγ9Vδ2 T-cells phenotyping across different tissue sites, related to Figure 2.

(figure legend on next page)

Figure S1: Vγ9Vδ2 T-cells phenotyping across different tissue sites, related to Figure 2. Vγ9Vδ2 T-cell phenotype was evaluated in peripheral blood mononuclear cells (PBMC), inguinal lymph nodes/tracheobronchial lymph nodes (ILN/TBLN), mesenteric lymph nodes (MLN), spleen, thymus, lung, and liver. **(A)** Representative histograms and frequencies of CCR5 (%), CCR6 (%), CXCR3 (%), and IL-18R (MFI) expression on Vγ9Vδ2 T-cells (n = 3-6 animals depending on tissue availability, from 3-5 independent experiments). **(B)** Representative histograms and expression frequencies of the transcription factor PLZF (%) on Vγ9Vδ2 T-cells (n = 3-6 animals depending on tissue availability and cell recovery, from 3-5 independent experiments). **(C)** Representative histograms and expression frequencies of the T_{fh} associated markers CXCR5 (%) and Bcl6 (%) on Vγ9Vδ2 T-cells (n = 3-6 animals depending on tissue availability and cell recovery, from 3-5 independent experiments). For CXCR5, samples were rested for 16hrs at 37°C and 5% CO_2 prior to FACS antibody labelling and data collection. **(D)** Representative histograms and expression frequencies of IL-17A (%) and GM-CSF (%) on Vγ9Vδ2 T-cells (n = 2-6 animals depending on tissue availability and cell recovery, from 2-5 independent experiments). Cytokine production frequencies were calculated following a 16hr *in vitro* stimulation with HMB-PP as described in the Method details, and the background subtracted from paired unstimulated control samples. **(E)** Representative histograms and expression frequencies of the transcription factors T-bet and Eomes (%) on Vγ9Vδ2 T-cells (n = 3-6 animals depending on tissue availability and cell recovery, from 3-5 independent experiments). **(F)** Representative histograms and expression frequencies of the cytotoxicity marker DNAM-1 (%) on Vγ9Vδ2 T-cells (n = 3-6 animals depending on tissue availability and cell recovery, from 3-5 independent experiments). Each point on the graphs represents an individual animal for each tissue sample. Lines and error bars indicate the median and interquartile range. All analysis was performed on cryopreserved PBMC and tissue samples. Statistics assessed by Kruskal-Wallis test with Dunn's multiple comparisons correction **(A-D, F)**. *p< 0.05, **p< 0.01

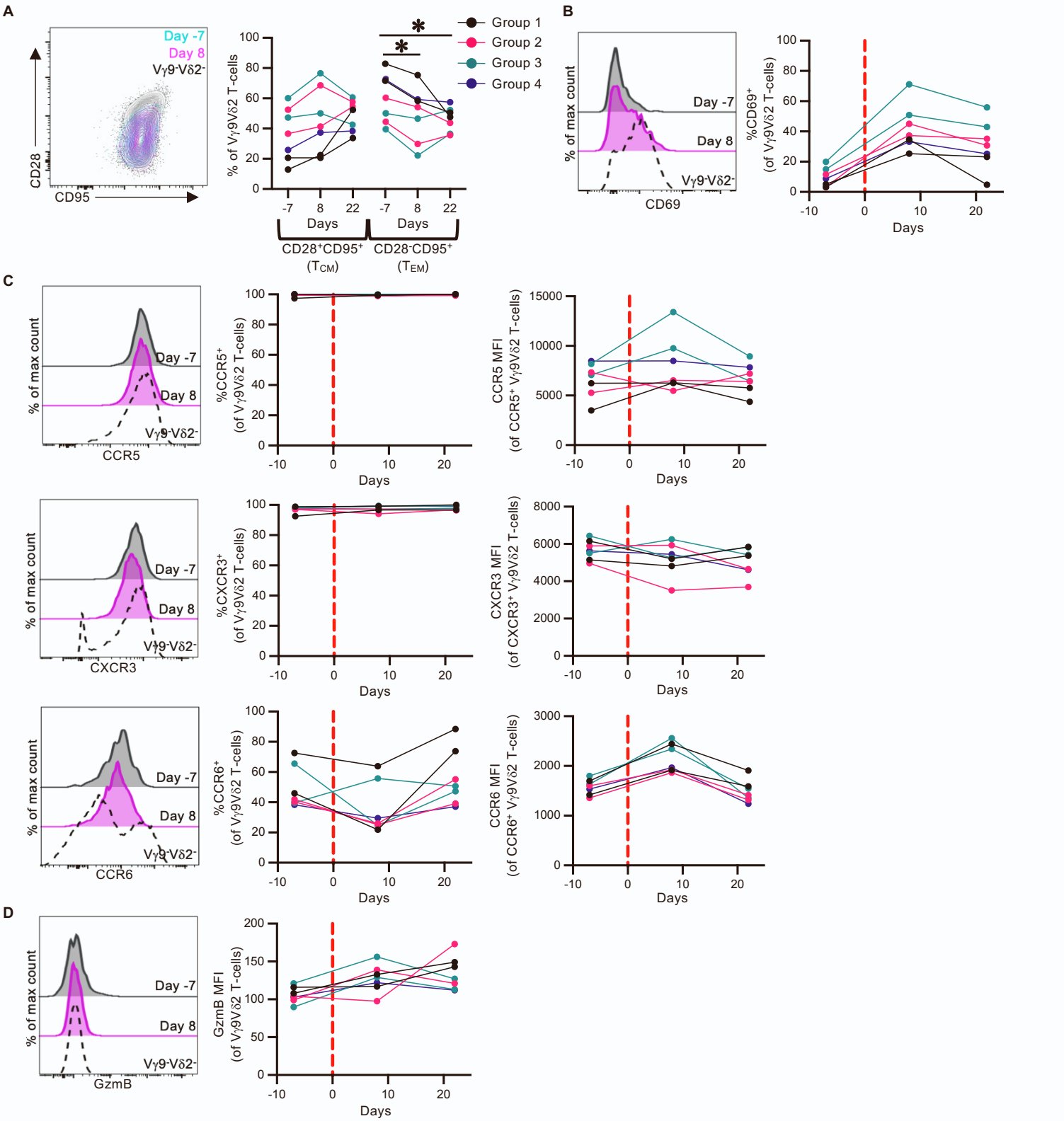

Figure S2: Phenotype of *in vivo* expanded Vγ9Vδ2 T-cells in bronchoalveolar lavage fluid (BAL), related to figure 4. Phenotyping was performed on freshly isolated BAL samples (n= 7 animals; 1-2 per treatment group). **(A)** Representative FACS plot and frequencies of central memory (T_{CM}; $CD28^+CD95^+$) and effector memory (T_{EM}; $CD28^-CD95^+$) Vγ9Vδ2 T-cells pre- and post-antigen administration. Expanded Vγ9Vδ2 T-cells (Day 8) are plotted in magenta, while pre-expanded Vγ9Vδ2 T-cells (Day -7) are plotted in cyan. Vγ9-Vδ2- T-cells are plotted in black. **(B)** Representative histograms and frequencies of CD69 expression on Vγ9Vδ2 T-cells pre- and post-antigen administration. **(C)** Representative histograms and frequencies of chemokine receptors CCR5, CCR6, and CXCR3 on Vγ9Vδ2 T-cells pre- and post-antigen administration. **(D)** Representative histograms and median fluorescence intensities (MFI) of granzyme B (GzmB) expression in Vγ9Vδ2 T-cells pre- and post-antigen administration. Each point on the graphs represents an individual animal from each timepoint. Data collected from 1 experiment. Statistics assessed by Friedman test with Dunn's multiple comparisons correction across all 4 groups **(A)**. *p< 0.05

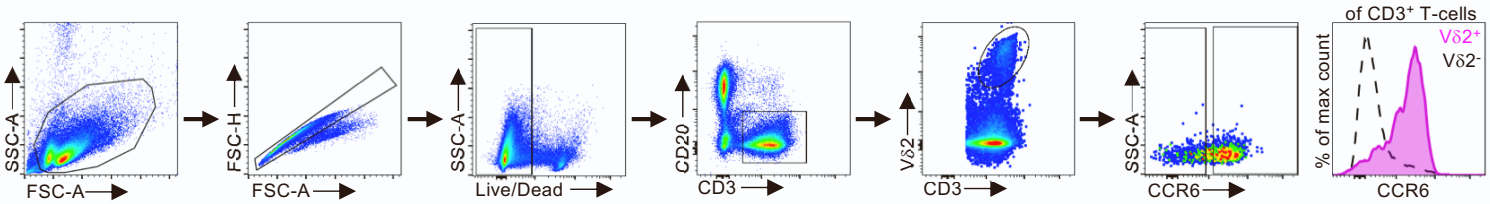

Figure S3: Gating strategy for CCR6 Sorted Vδ2⁺ T-cells, related to Figure 5. CCR6⁺ and CCR6⁻ CD3⁺Vδ2⁺ were identified for sort purification using the indicated gating strategy. The histogram illustrates the CCR6 expression on Vδ2⁺ (magenta) and Vδ2⁻ (black) T-cells, which was used to determine the CCR6 sort gate placement.

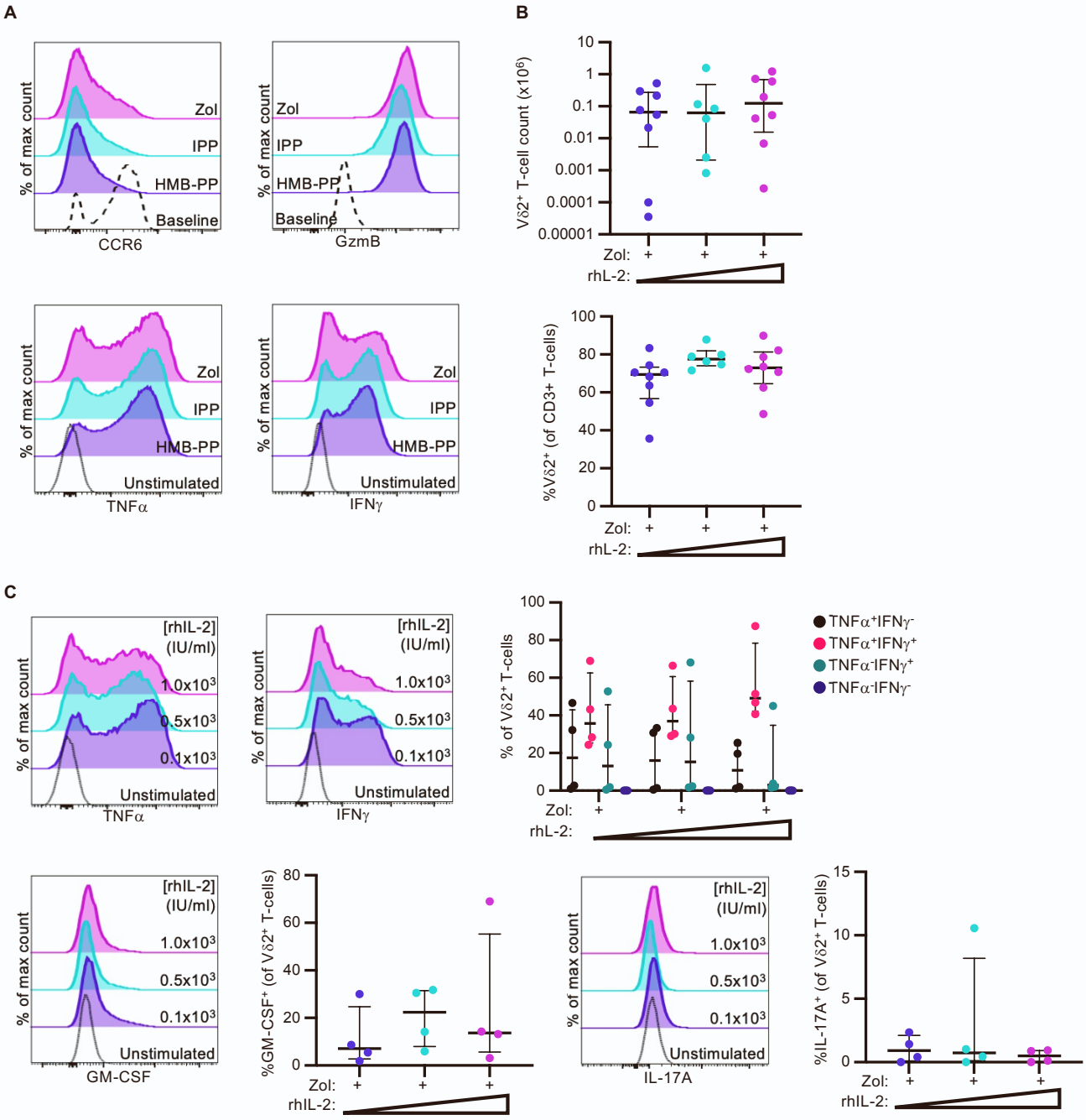

Figure S4: Phenotypic changes in pigtail macaque Vδ2⁺ T-cells following *in vitro* expansion, related to Figure 6. (A) Representative histograms of CCR6, Granzyme B (GzmB), TNFα, and IFNγ expression on *in vitro* expanded Vδ2⁺ T-cells (n = 3 animals from 2 independent experiments). Cultures were expanded with rhIL-2 (1 x10³ IU/mL) and Zol (15μM), IPP (4μg/mL), or HMB-PP (20ng/mL) for 13 days. (**B**) Absolute Vδ2⁺ T-cell counts and Vδ2⁺ T-cell frequencies as a percentage of total CD3⁺ T-cells (n = 6-8 animals from 4 independent experiments). **(C)** Representative histograms and frequencies of IFNγ (%), TNFα (%), GM-CSF (%), and IL-17A (%) expression on *in vitro* expanded Vδ2⁺ T-cells (n = 4 animals from 2 independent experiments). All expansions were performed with cryopreserved pigtail macaque peripheral blood mononuclear cells over a 13-day expansion period. All intracellular cytokine stimulation assays were performed on mitogenically stimulated Vδ2⁺ T-cells, as described in the Method details. Cytokine production frequencies were calculated following background subtraction using paired unstimulated control samples. Each point on the graphs represents an individual animal for each expansion condition. Lines and error bars indicate the median and interquartile range. Statistics assessed by Kruskal-Wallis test with Dunn's multiple comparisons correction (**B**) or Friedman test with Dunn's multiple comparisons correction (**C**).

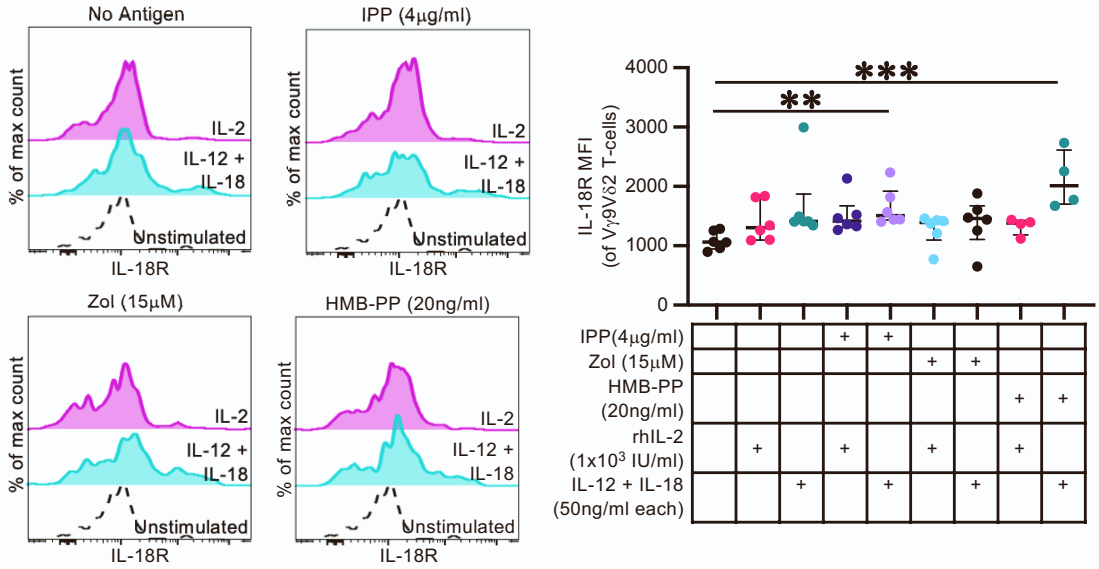

Figure S5: Phenotypic changes in pigtail macaque Vγ9Vδ2 T-cells following acute *in vitro* stimulation, related to Figure 6. Representative frequencies of IL-18R (MFI) expression on *in vitro* stimulated Vγ9Vδ2 T-cells (n = 4-7 per group from 3 independent experiments) that were incubated for 72hrs with the indicated stimuli prior to evaluation. Each point on the graph represents an individual animal for each stimulation condition Lines and error bars indicate the median and interquartile range. Statistics assessed by the Kruskal-Wallis test with Dunn's multiple comparisons correction. **p< 0.01, ***p< 0.001

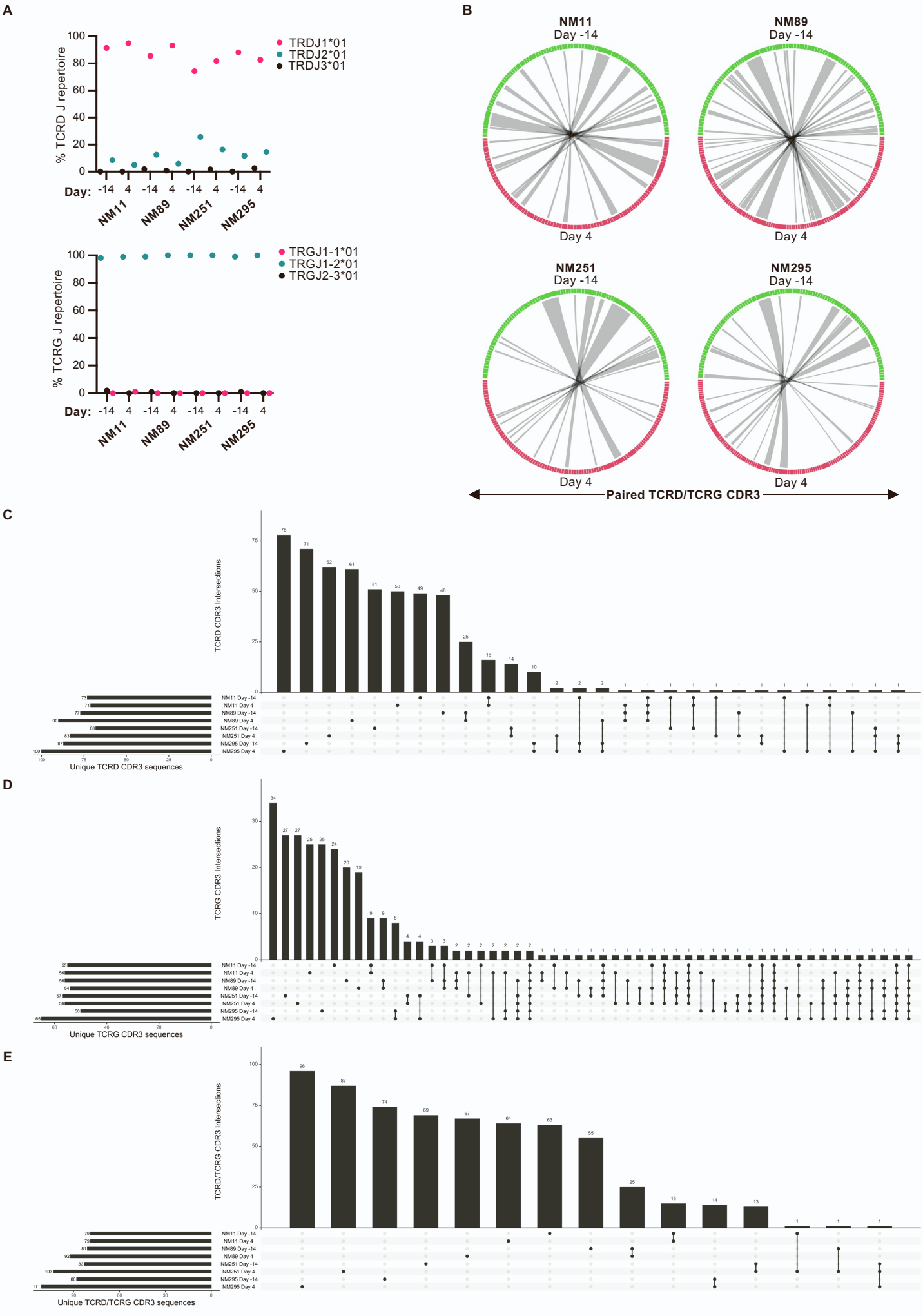

Figure S1: Peripheral blood Vγ9Vδ2 clonality and clonal sharing between individuals, related to Figure 7

(figure legend on next page)

Figure S6: Peripheral blood Vγ9Vδ2 clonality and clonal sharing between individuals, related to Figure 7: **(A)** TCRD and TCRG J-chain usage within pigtail macaque Vγ9Vδ2 T-cells pre-expansion (Day -14) and during peak *in vivo* expansion (Day 4). J-chain usage is presented as a percentage of the total chain recovery for each animal at each timepoint, and TRDJ/TRGJ chains are labelled according to IMGT allele names (species: *Macaca mulatta*). **(B)** Normalized, paired TCRD/TCRG clonotype sharing between pre-expanded (day -14) and expanded (day 4) samples in individual animals. **(C-E)** UpSet plots illustrating individual TCRD **(C)**, TCRG **(D)**, and paired TCRD/TCRG **(E)** clonotype sharing within individual animals and between animals.

Table S1: Vγ9Vδ2 T-cell diversity following *in vivo* pharmacological expansion, related to Figure 7.

		Number of reads		Richness					Simpson's diversity index			
	Animal ID	T1[a]	T2[b]	T1	T2	|T2 - T1|	*p*-value[c]	Shared clones[d]	T1	T2	|T2 - T1|	*p*-value[c]
TCRD	NM11	106	99	73	71	2	0.7400	19	0.979	0.979	2.94E-04	0.9460
	NM89	104	135	77	90	13	0.6959	27	0.979	0.982	0.003	0.5169
	NM251	109	116	68	83	15	0.0531	15	0.962	0.973	0.011	0.1582
	NM295	110	147	87	100	13	0.9279	15	0.983	0.982	0.001	0.7870
TCRG	NM11			55	56	1	0.8297	17	0.958	0.958	5.13E-04	0.9577
	NM89			56	54	2	0.8811	27	0.970	0.961	0.09	0.2459
	NM251			57	56	1	0.8325	19	0.957	0.940	0.017	0.0979
	NM295			50	65	15	0.3092	18	0.920	0.953	0.033	0.0535
TCRD/TCRG	NM11			79	79	0	0.9504	15	0.981	0.982	0.001	0.7964
	NM89			81	92	11	0.8419	25	0.982	0.983	0.001	0.7717
	NM251			83	103	20	0.0042	14	0.976	0.988	0.012	0.0022
	NM295			88	111	23	0.6203	14	0.984	0.985	0.001	0.6832

[a] T1: Day -14
[b] T2: Day 4
[c] *p*-values were calculated using the randomization test, where the *p*-value for the difference in diversity is the probability that a randomly distributed pool of CDR3 sequences between the 2 timepoints would have a difference in richness/Simpson's diversity index greater than the actual difference (n = 10,000 random CDR3 distributions).
[d] Number of shared unique clones between T1 and T2

Table S2: R package usage for TCR sequencing analysis, related to STAR Methods Section.

Analysis	R package (version)	Publication
Alluvial plots	ggalluvial (v0.12.3)	Brunson, 2020 [S1]
Sequence logo	msa (v1.26.0)[a]	Bodenhofer et al., 2015 [S2]
Simpson Diversity Index, Richness	vegan (v2.6-2)	Jari Oksanen, et al. (2022). vegan: Community Ecology Package. https://CRAN.R-project.org/package=vegan [S3]
Randomization test	parallel	R Core Team (2022). R: A language and environment for statistical computing. R Foundation for Statistical Computing, Vienna, Austria. URL https://www.R-project.org/ [S4]
Circos plots	circlize (v0.4.15)	Gu et al., 2014 [S5]
UpSet plots	UpSetR (v1.4.0)	Conway et al., 2017 [S6]
Miscellaneous	Tidyverse (v1.3.1)	Wickham et al., 2019 [S7]

[a] Sequence alignments performed with the “ClustalW” alignment algorithm

Supplemental references:

[S1] Brunson, J. (2020). ggalluvial: Layered Grammar for Alluvial Plots. J Open Source Softw *5*, 2017. 10.21105/joss.02017.

[S2] Bodenhofer, U., Bonatesta, E., Horejš-Kainrath, C., and Hochreiter, S. (2015). msa: an R package for multiple sequence alignment. Bioinformatics *31*, 3997–3999. 10.1093/bioinformatics/btv494.

[S3] Oksanen, J., Simpson, G.L., Blanchet, F.G., Kindt, R., Legendre, P., Minchin P.R., O'Hara, R.B., Solymos, P., Stevens, M.H., Szoecs, E., Wagner, H., Barbour, M., Bedward, M., Bolker, B., Borcard, D., Carvalho, G., Chirico, M., De Caceres, M., Durand, S., Antoniazi Evangelista, H.B., FitzJohn, R., Friendly, M., Furneaux, B., Hannigan, G., Hill, M.O., Lahti, L., McGlinn, D., Ouellette, M-H., Cunha, E.R., Smith, T., Stier, A., Ter Braak, C.J.F., and Weedon, J. (2022). vegan: Community Ecology Package. https://CRAN.R-project.org/package=vegan

[S4] R Core Team (2022). R: A language and environment for statistical computing. R Foundation for Statistical Computing, Vienna, Austria. URL https://www.R-project.org/

[S5] Gu, Z., Gu, L., Eils, R., Schlesner, M., and Brors, B. (2014). circlize implements and enhances circular visualization in R. Bioinformatics *30*, 2811–2812. 10.1093/bioinformatics/btu393.

[S6] Conway, J.R., Lex, A., and Gehlenborg, N. (2017). UpSetR: an R package for the visualization of intersecting sets and their properties. Bioinformatics *33*, 2938–2940. 10.1093/bioinformatics/btx364.

[S7] Wickham, H., Averick, M., Bryan, J., Chang, W., McGowan, L., François, R., Grolemund, G., Hayes, A., Henry, L., Hester, J., et al. (2019). Welcome to the Tidyverse. J Open Source Softw *4*, 1686. 10.21105/joss.01686.